Journal of Solid State Chemistry 184 (2011) 3062–3065

Contents lists available at SciVerse ScienceDirect

Journal of Solid State Chemistry

journal homepage: www.elsevier.com/locate/jssc

The role of TiO_2 in the B_2O_3–Na_2O–PbO–Al_2O_3 glass system

N.C.A. de Sousa [a], M.T. de Araujo [a], C. Jacinto [a], M.V.D. Vermelho [a], N.O. Dantas [b], C.C. Santos [c], I. Guedes [d,*]

[a] Instituto de Física, Universidade Federal de Alagoas, 57072-970 Maceió, AL, Brazil
[b] Laboratório de Novos Materiais Isolantes e Semicondutores (LNMIS), Instituto de Física, Universidade Federal de Uberlândia, 38400-902 Uberlândia, MG, Brazil
[c] Departamento de Física, CCET, Universidade Federal do Maranhão, 65085-580 São Luis, MA, Brazil
[d] Departamento de Física, Universidade Federal do Ceará, Campus do PICI, Caixa Postal 6030, 60455-760 Fortaleza, CE, Brazil

ARTICLE INFO

Article history:
Received 26 March 2011
Received in revised form
22 August 2011
Accepted 14 September 2011
Available online 21 September 2011

Keywords:
Raman spectra
Infrared spectra
Glass

ABSTRACT

Optical and vibrational studies have been carried out on $60B_2O_3 \cdot (20-x)Na_2O \cdot 10PbO \cdot 10Al_2O_3{:}xTiO_2$ ($x=0$, 1, 2, 3, 4, and 5 mol%) glasses, in order to understand the role of TiO_2 in the $60B_2O_3 \cdot 20Na_2O \cdot 10PbO \cdot 10Al_2O_3$ glass matrix. The X-ray patterns reveal homogeneous glasses over the entire compositional range. The absorption spectra show that the energy of the optical band gap (ΔE_{opt}) and Urbach's energy (E_U) decreases as TiO_2 content increases. The changes observed in the Raman and IR spectra are related to the $BO_4 \rightarrow BO_3$ back conversion effect and the appearance of "loose" BO_4^- groups. The data indicate that titanium ions act as a network modifier.

1. Introduction

Borate-based (B_2O_3-based) glasses have been investigated over the last years due to their variety of engineering applications. Usually B_2O_3-based glasses are highly transparent in both visible and near-infrared regions and can be produced over a large compositional range [1].

Borate glasses containing alkali or alkali earth oxides exhibit high mechanical strength and are relatively moisture-resistant when compared with the pure borate glasses. Some of their applications include phosphors, solar energy converters and optical devices [2]. The addition of either lead oxide (PbO) or aluminum oxide (Al_2O_3) to B_2O_3-based glasses improves their chemical durability. Incorporation of Al_2O_3 to B_2O_3-based glasses reduces the glass transition temperature (T_g), increases the thermal expansion coefficient, and reduces the molar volume [3]. While the PbO–B_2O_3 glasses are very promising candidates to be used in optics and optoelectronics [4], the Al_2O_3–B_2O_3-based glasses find industrial applications as sealing glasses, separators in batteries and dental cement components [5,6].

It is well known that the addition of transition-metal oxides to B_2O_3-based glasses changes their chemical and physical properties. For instance, incorporation of titanium oxide (TiO_2) to a glass matrix not only improves its chemical durability but also increases its nonlinear refractive index, once the empty or unfilled *d*-shell of Ti ions contribute more strongly to the nonlinear polarizability. Therefore, TiO_2:B_2O_3-based glasses can be very promising candidates to be used as nonlinear optical devices [7,8]. Depending upon its concentration, the transition-metal oxide may act either as a network modifier or as a network former.

The role of titanium ions on the physical properties of B_2O_3-based glasses have been investigated by Maniu et al. [9] and Balaji Rao et al. [10] in the systems $3B_2O_3 \cdot K_2O$ and $Li_2O \cdot MgO \cdot B_2O_3$, respectively. The $3B_2O_3 \cdot K_2O$ glass contains mainly pentaborate groups and boroxol rings. From Raman measurements, Maniu et al. [9] observed no changes for low TiO_2 content ($x \leq 0.1$). Further addition of TiO_2 led to the appearance of ring type metaborate groups and "loose" BO_4^- tetrahedra, which increases the number of non-bridging oxygens. They concluded that the titanium ions act as network modifier. Using several techniques Rao et al. [10] showed that when the concentration of TiO_2 in the glass network $Li_2O \cdot MgO \cdot B_2O_3$ is ≤ 0.4 mol%, titanium ions exist in Ti^{4+} state and act as network formers.

The present investigation is intended to provide a comprehensive understanding of the role of TiO_2 on the optical and vibrational properties of the quaternary $60B_2O_3 \cdot 20Na_2O \cdot 10PbO \cdot 10Al_2O_3$ glass system, where TiO_2 replaces for Na_2O. We will show that the TiO_2 plays the role as glass-modifier and influences on the $BO_4 \rightarrow BO_3$ back conversion effect.

2. Experimental

The glasses were prepared by the conventional melt quenching method. The starting materials purchased from Aldrich Chemical Co., B_2O_3 (99.9%), Na_2O (99.5%), PbO (99.9%), Al_2O_3 (99.5%), and TiO_2 (99.5%) were taken in appropriate proportions and ground

* Corresponding author. Fax: +55 85 3366 9450.
E-mail address: guedes@fisica.ufc.br (I. Guedes).

0022-4596/$ - see front matter © 2011 Elsevier Inc. All rights reserved.
doi:10.1016/j.jssc.2011.09.011

Table 1
The nominal composition of the glass system $60B_2O_3 \cdot (20-x)Na_2O \cdot 10PbO \cdot 10Al_2O_3{:}xTiO_2$, along with their codes, ρ , ΔE_{opt}, and E_U.

Code	Composition (mol%)					Density (ρ) (g/cm^3)	ΔE_{opt} Allowed (eV)	E_U (eV)
	B_2O_3	Na_2O	PbO	Al_2O_3	TiO_2			
BNPA0T	60	20	10	10	0	2.80	3.28	0.613
BNPA1T	60	19	10	10	1	2.83	3.41	0.544
BNPA2T	60	18	10	10	2	2.76	3.37	0.406
BNPA3T	60	17	10	10	3	2.78	3.38	0.353
BNPA4T	60	16	10	10	4	2.77	3.24	0.377
BNPA5T	60	15	10	10	5	2.78	3.12	0.405

together to constitute a 10 g batch. The ground mixtures were heated in crucibles at 1300 °C for 1 h in a muffle furnace. The batches were then melted at 1300 °C for 1 h, stirred to ensure homogeneity, and quenched between stainless steel plates kept at 350 °C for 24 h. Table 1 shows the nominal composition of the glasses along with their codes, density (ρ), energy of the optical band gap (ΔE_{opt}), and Urbach's energy (E_U).

The X-ray diffraction (XRD) patterns were recorded using a XRD-6000 Shimadzu diffractometer with Cu-$K\alpha$1 radiation (λ=1.54056 Å). The density of glass system was measured by the conventional Archimedes' method using distilled water as immersion liquid (ρ=0.9971 at 25 °C).

The optical absorption spectra were measured using a white light (LS-1 tungsten halogen lamp—Ocean Optics, Inc.) radiation source and a 0.67 m McPherson scanning spectrograph (resolution of 0.1 nm). The Raman spectra were recorded with a Jobin-Yvon T64000 triple-grating spectrometer using the 514.5 nm excitation line from an Ar^+ laser (Coherent Inc., Innova 70). The spectra were collected in back-scattering geometry with a resolution of 2 cm^{-1}. Detection of the Raman signal was carried out with a N_2-cooled CCD. The Fourier Transform infrared (FT-IR) absorption spectra were recorded on a Bruker VERTEX 70 FT-IR spectrometer (resolution of 4 cm^{-1}), in the mid-region (400–4000 cm^{-1}), using the KBr pallet technique, and the signal was acquired using a DigiTect DLaTGS detector with an integrated preamplifier. The X-ray, optical absorption, Raman and IR measurements were recorded at room temperature.

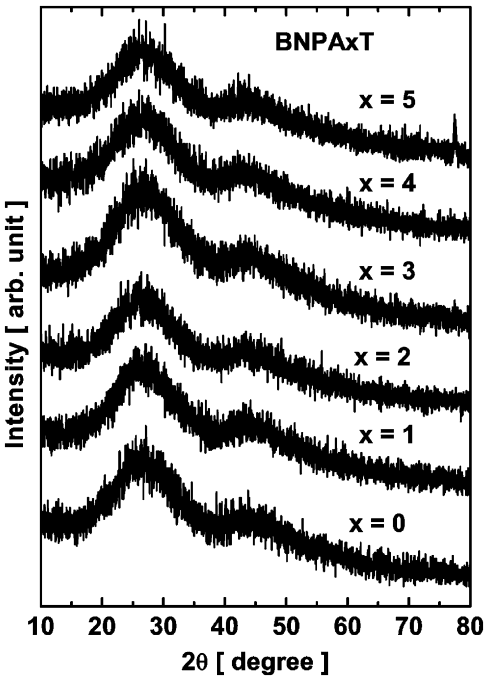

Fig. 1. X-ray diffraction patterns of the $60B_2O_3(20-x) \cdot Na_2O \cdot 10PbO \cdot 10Al_2O_3 \cdot xTiO_2$ (x=0, 1, 2, 3, 4, and 5 mol%) glasses.

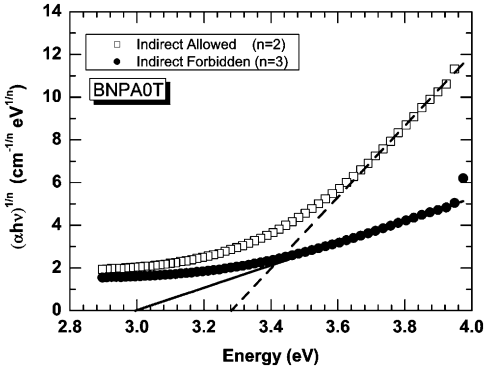

Fig. 2. Typical plot of the $(\alpha h\nu)^{1/n}$ versus $h\nu$ along with the ΔE_{opt} values for BNPA0T glasses were obtained.

3. Results and discussion

The XRD patterns of the glass samples are shown in Fig. 1. The two broaden diffraction lines reveal the amorphous nature of all prepared samples. Information on the incorporation of TiO_2 into the glass structure can be obtained from the optical spectrum, which provides a very useful tool for the investigation of optically induced transition and an insight into the energy gap and band structure of solid state materials.

Mott and Davis [11] related the absorption coefficient to the electronic energy band gap through the following relation:

$$\alpha(\omega) = (B(\hbar\omega - \Delta E_{opt})^n)/\hbar\omega \quad (1)$$

where B is a constant, ΔE_{opt} is the optical band gap energy and n may have the following values 2, 3, 1/2 and 1/3 depending on the interband electronic transition. These values of n can be understood in the framework of the ligand field theory. The indirect and direct forbidden transitions (n=3 and 1/3, respectively) are attributed to weak absorption bands within the d-levels of the transition elements. Despite the fact that these transitions are forbidden by Laporte's rule, the electric dipole transition coupled with molecular vibrations relax this rule, allowing the electronic transitions to occur. The strong absorption bands (n=2 and 1/2) can be roughly viewed as a transfer of the charge from the ligands to the central ion consisting of transition metal. These transitions are allowed by Laporte's rule, and their intensity is stronger than those of the forbidden transitions. The experimental data were linearized according to the four possible transition mechanisms described above and the straight lines were fitted minimizing the errors (R^2). The typical result is depicted in Fig. 2.

Two indirected transitions were observed: an indirect allowed (assisted by phonons) transition, n=2, and an indirect forbidden transition, n=3. From the plot of $(\alpha h\nu)^{1/n}$ versus $h\nu$, we obtain a straight line in the neighborhood of optical absorption edge. The extrapolation of the line to the energy axis with α=0, yields the value of ΔE_{opt}, which for BNPAxT (x=0,…,5) glasses are listed in Table 1. We observe that ΔE_{opt} decreases (7.2%) with increasing the TiO_2 concentration.

In Ref. [12], it was observed that partial replacement of either PbO or P_2O_5 by Sb_2O_3 in the $(PbO)_{0.4}(P_2O_5)_{0.6}$ base glass reduces ΔE_{opt}. This is likely to be related to the increase in the number of non-bridging oxygen atoms owing to the increase in Q^2 structural units of phosphorus ionically bonded to Pb^{2+}. The negative

charge of non-bridging oxygen atoms reduces the energy required for the excitation of electron reducing ΔE_{opt}.

According to Ref. [11], the width of the tail of the absorption spectra can also be used to analyze possible changes in the glass structure. Following the Urbach's rule [13], the optical absorption coefficient $\alpha(\omega)$ exhibits an exponential increase and is given by

$$\alpha(\omega) = \alpha_0 \exp(\hbar\omega/\Delta E) \quad (2)$$

where α_0 is a constant, $\hbar\omega$ is the photon energy, and ΔE is the Urbach's energy (E_U) accounting for the width of the tail of localized states.

The values of E_U obtained from Fig. 2 are listed in Table 1 and plotted in Fig. 3. We observe that E_U reduces by 40% when TiO_2 content goes from 0 to 5 mol%, indicating that the BNPA structure changes with increasing TiO_2 content. The changes can be probed by Raman and IR spectroscopy.

The Raman spectra of the BNPAxT glasses are shown in Fig. 4. Besides BO_3 and BO_4 groups, complex borate glasses consist of relatively large structural units, such as boroxol, pentaborate, triborate, diborate and metaborate groups with bridging and non-bridging oxygen ions. Consider the spectrum for $x=0$ (BNPA0T). It consists of 5 relatively broad bands. The low intensity band centered at $\sim 300\ cm^{-1}$ is likely to be assigned as vibrations of PbO units [14]. The band spanning the 400–600 cm^{-1} region should contain the B–O–B stretching vibrations of the BO_4 units [15]. The band appearing in the 630–830 cm^{-1} region contains the vibration assigned to chain-type metaborate groups at $\sim 755\ cm^{-1}$ (#1) [16,17], the symmetric breathing vibration of six-membered rings with one BO_4 tetrahedron (triborate, tetraborate or pentaborate) at $\sim 772\ cm^{-1}$ (#2) [16], and the characteristic boroxol ring oxygen breathing vibration at $\sim 797\ cm^{-1}$ (#3) [18,19]. The band appearing in the 850–1100 cm^{-1} range results from the B–O–B stretching vibration (830–850 cm^{-1}) of pyroborate groups, the B–O vibration (890–940 cm^{-1}) of orthoborate groups, and the B–O or B–O–B stretching vibration (1075–1150 cm^{-1}) of diborate groups [15]. The last band centered at about $\sim 1400\ cm^{-1}$ is due to the B–O stretching (1200–1300 cm^{-1}) of pyroborate groups and the B–O vibrations (1300–1600 cm^{-1}) of both chain and ring metaborate groups [15].

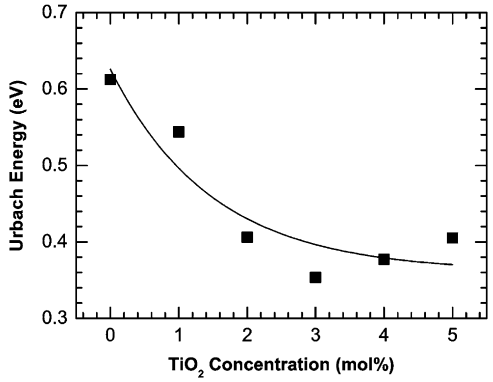

Fig. 3. Dependence of the Urbach's Energy (E_U) with the TiO_2 concentration. The solid line is just to guide the eyes.

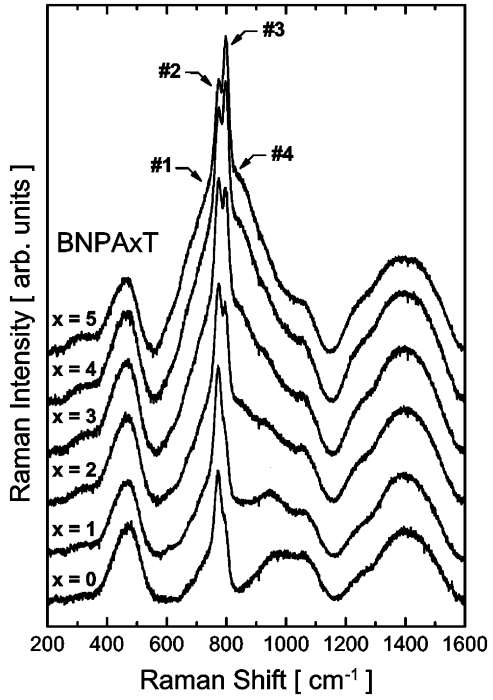

Fig. 4. Raman spectra of BNPA:xTiO$_2$ (x=0, 1, 2, 3, 4, and 5) glasses.

As the TiO_2 content increases two main features are observed: (i) the intensity of the band #3 becomes higher than that of the band #2 and (ii) the appearance of a shoulder at $\sim 835\ cm^{-1}$ (#4) that becomes very intense for $x=5$ mol% (BNPA5T).

The ratio between the intensity of the bands #2 and #3 ($I_{\#2}/I_{\#3}$) has been reported to change depending on the alkali oxide content. The introduction of an alkali oxide into B_2O_3 glass leads to the conversion of sp^2 planar BO_3 units into more stable sp^3 tetrahedral BO_4 units, along with the creation of non-bridging oxygens. Akagi et al. [20] investigated the structures of xK$_2$O–$(1-x)$B$_2$O$_3$ glasses and melts by Raman spectroscopy. They observed that $I_{\#2} < I_{\#3}$ for $x=10$ mol%, while $I_{\#2} > I_{\#3}$, for $x=20$ and 30 mol% at 300 K. Similar results were reported by Yano et al. [21] for xNa$_2$O–$(1-x)$B$_2$O$_3$ glasses.

The effect of alkali earth oxides on the structure of B_2O_3 glass was investigated by Maniu et al. [22]. They observed that the structure of the $(1-x)$CaO–xB$_2$O$_3$ glasses changes with increasing the CaO content. For $x=0.8$ the main structural unit is the boroxol ring ($I_{\#3} > I_{\#2}$) and ring-based units. For $x < 0.7$ they observed that $o_{\#3} < I_{\#2}$; the structure being composed mainly of pentaborate and orthoborate groups. It means that as the CaO content increases, the boroxol ring and pentaborate units are gradually open to form chain-type metaborate groups and orthoborate groups.

Maniu et al. [9] have also investigated the influence of TiO_2 on the structure of K_2O–$3B_2O_3$ glass. They recorded the Raman spectra of the $(1-x)$[K$_2$O–3B$_2$O$_3$]–xTiO$_2$ glasses with $0 \le x \le 0.5$. For $x=0$, they observed bands at $\sim$420, $\sim$475, $\sim$670, $\sim$770, $\sim$800, $\sim$930, $\sim$1230, and $\sim 1450\ cm^{-1}$. The bands at $\sim$420, $\sim$475, $\sim$670, $\sim$930, and 1450 cm^{-1} were assigned to the asymmetric vibration of "loose" BO_4^- tetrahedra, the ring angle bending (B–O–B) of borate units, vibrations of metaborate units, vibrations of pentaborate units, and vibrations of the chain-type metaborate groups, respectively. For $0 < x \le 0.1$, they observed no significant change either in the frequency or intensity of the bands, which indicates that low concentration of titanium does not modify the glass structure. For $x > 0.2$, they observed an increase in the intensity of the bands at $\sim$420, $\sim$475 and $\sim 670\ cm^{-1}$. For $x=0.5$, they noted the appearance of two shoulders at $\sim$600 and $\sim 850\ cm^{-1}$. The band at $\sim 850\ cm^{-1}$ was assigned to the asymmetric vibration of "loose" BO_4^- tetrahedron. The addition of titanium ions determines the appearance of "loose" BO_4^- tetrahedra, that increases the number of non-bridging oxygens. They concluded that the titanium ions act as network modifiers for $x \ge 0.2$.

Based on the above results, the band at $\sim 835\ cm^{-1}$ is likely to be due to the presence of "loose" BO_4^- groups. The change in the ratio ($I_{\#2}/I_{\#3}$) is likely to be related to the so-called $BO_4 \rightarrow BO_3$ back conversion [23–25], since the addition of TiO_2 decreases the alkali (Na_2O) content. In the $BO_4 \rightarrow BO_3$ back conversion, the

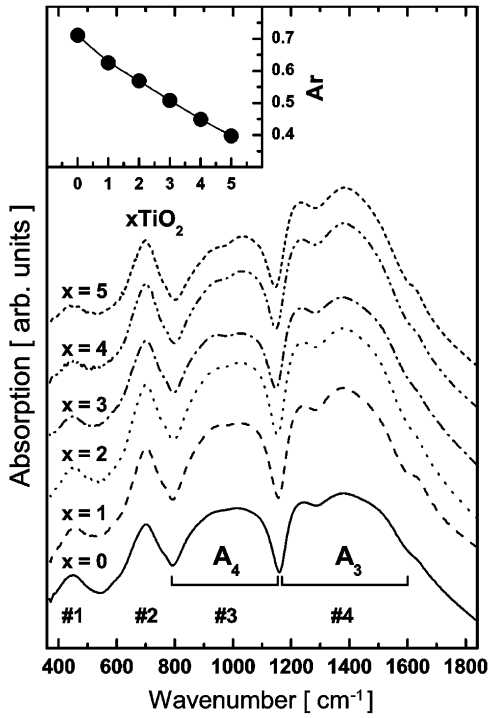

Fig. 5. FT-IR spectra of BNPA:xTiO$_2$ (x=0, 1, 2, 3, 4, and 5) glasses. The inset shows the Ar ($=A_4/A_3$) ratio.

number of non-bridging oxygen ions increases, which agrees with the trend presented by ΔE_{opt}.

The $BO_4 \rightarrow BO_3$ back conversion can be better observed from the IR spectra, shown in Fig. 5. For x=0, we observe four absorption bands at around ~480 (#1), ~700 (#2), ~1000 (#3), and ~1350 (#4) cm^{-1}. Similar spectra were observed by Pisarski et al. [26] for the system $(73.5-x)$PbO–18.5B_2O_3–5Al_2O_3–3WO_3–$x$$Ln_2O_3$(Ln=Nd, Er), Ciceo-Lucacel and Ardelean [1] for the system xMnO$\cdot(100-x)$[3B_2O_3–0.9PbO–0.1Ag_2O], Saddeek for the system $Na_{2-2x}B_{4-4x}Pb_xO_{7-6x}$ [27], El-Fayoumi and Farouk for the system $x$$Sm_2O_3+(100-x)$[0.84$B_2O_3$+0.15$Li_2O$+0.01$Eu_2O_3$] [28], Balaji Rao et al. for the system Li_2O–MgO–B_2O_3:TiO_2 [10], and Bengisu et al. [29] for the systems SrO–TiO_2–Al_2O_3–B_2O_3:P_2O_5 and SrO–TiO_2–Al_2O_3–SiO_2:P_2O_5. Following the assignment given in Ref. [26] we identify the band #1 as the B–O–B and Pb–O–B bending vibrations as well as borate ring deformations, the band #2 as the bending vibrations of the BO_3 group, the band #3 as the B–O stretching vibrations of the tetrahedral BO_4 group, and the band #4 as the asymmetric B–O stretching vibrations of the trigonal BO_3 group.

Let A_3 and A_4 be the integrated intensity of the BO_3 (1150–1600 cm^{-1}) and BO_4 (790–1150 cm^{-1}) vibrations, respectively. The integrated intensity is calculated as the integral of the absorption signal using the software OPUS 6.5 available in the VERTEX 70 FT-IR spectrometer. The relative integrated intensity Ar$=A_4/A_3$ can be used to quantify the effect of the incorporation of the TiO_2 into the structure of the glasses, as shown in the inset of Fig. 5. We observe that Ar decreases by 45% with increasing TiO_2 content, indicating that the number of BO_4 groups is decreasing due to the $BO_4 \rightarrow BO_3$ back conversion. It should be noted the correspondence between the reduction of the BO_4 groups (45%) with the reduction of E_U (40%).

4. Conclusion

A quaternary $60B_2O_3\cdot 20Na_2O\cdot 10PbO\cdot 10Al_2O_3$ glass system containing TiO_2 have been studied by XRD, optical absorption, Raman and IR techniques. The XRD data show the amorphous character of all $60B_2O_3\cdot(20-x)Na_2O\cdot 10PbO\cdot 10Al_2O_3$:$xTiO_2$ (x=0, 1, 2, 3, 4, and 5 mol%) glasses. The optical absorption measurements indicate that the Urbach's energy reduces by 40% when TiO_2 content goes from 0 to 5 mol%, evidencing a possible change of the glass structure. The Raman data show the following modifications: the appearance of a band (~850 cm^{-1}) related to the asymmetric vibration of "loose" BO_4^- tetrahedron, and the change in the ratio $I_{\#2}/I_{\#3}$ which is related to the so-called $BO_4 \rightarrow BO_3$ back conversion, as verified from IR data. The $BO_4 \rightarrow BO_3$ back conversion and the increase in the number of non-bridging oxygen ions accounts for the trend observed for E_U and ΔE_{opt}. The overall results indicate that titanium (at least, up to 5 mol%) acts as a network modifier in the $60B_2O_3\cdot 20Na_2O\cdot 10PbO\cdot 10Al_2O_3$ glasses.

Acknowledgments

The financial support for this research by FINEP, CNPq, CAPES, Brazilian Agencies, are gratefully acknowledged. One of the authors N.C.A.S. is supported by graduate studentship from CNPq. C.C. Santos acknowledges the financial support from FAPEMA-MA-Brazil.

References

[1] R. Ciceo-Lucacel, I. Ardelean, J. Non-Cryst. Solids 353 (2007) 2020.
[2] D.L. Griscom, Borate Glass: Structure, Properties and Applications, Plenum, New York, 1978.
[3] I.N. Chakraborty, D.E. Day, J. Am. Ceram. Soc. 68 (1985) 641.
[4] D.W. Hall, M.A. Newhouse, N.F. Borrelli, W.H. Dumbaugh, D.L. Weidman, Appl. Phys. Lett. 54 (1989) 1293.
[5] R.K. Brow, D.R. Tallant, J. Non-Cryst. Solids 222 (1997) 396.
[6] A.D. Neve, V. Piddock, E.C. Combe, Clin. Mater. 12 (1993) 113.
[7] M. Sheikbahae, D.C. Hutchings, D.J. Hagan, E.W. Vanstryland, IEEE J. Quantum Electron. 27 (1991) 1296.
[8] Y. Watanabe, M. Ohnishi, T. Tsuchiya, Appl. Phys. Lett. 66 (1995) 3431.
[9] D. Maniu, I. Ardelean, T. Iliescu, S. Cinta, V. Nagel, W. Kiefer, J. Mol. Struct. 481 (1999) 657.
[10] R.B. Rao, D.K. Rao, N. Veeraiah, Mater. Chem. Phys. 87 (2004) 357.
[11] N.F. Mott, E.A. Davis, Philos. Mag. 17 (1968) 1269.
[12] V. Sudarsan, S.K. Kulshreshtha, J. Non-Cryst. Solids 286 (2001) 99.
[13] F. Urbach, Phys. Rev. 92 (1953) 1324.
[14] M. Ganguli, K.J. Rao, J. Solid State Chem. 145 (1999) 65.
[15] R.K. Brow, D.R. Tallant, G.L. Turner, J. Am. Ceram. Soc. 80 (1997) 1239.
[16] T.W. Bril, Raman-Spectroscopy of Crystalline and Vitreous Borates, Philips Research Report, 1976.
[17] E.I. Kamitsos, M.A. Karakassides, Phys. Chem. Glasses 30 (1989) 19.
[18] F.L. Galeener, Solid State Commun. 44 (1982) 1037.
[19] B.N. Meera, A.K. Sood, N. Chandrabhas, J. Ramakrishna, J. Non-Cryst. Solids 126 (1990) 224.
[20] R. Akagi, N. Ohtori, N. Umesaki, J. Non-Cryst. Solids 293 (2001) 471.
[21] T. Yano, N. Kunimine, S. Shibata, M. Yamane, J. Non-Cryst. Solids 321 (2003) 137.
[22] D. Maniu, T. Iliescu, I. Ardelean, S. Cinta-Pinzaru, N. Tarcea, W. Kiefer, J. Mol. Struct. 651 (2003) 485.
[23] A.E. Burns, D.W. Winslow, W.J. Clarida, M. Affatigato, S.A. Feller, R.K. Brow, J. Non-Cryst. Solids 352 (2006) 2364.
[24] S. Sindhu, S. Sanghi, A. Agarwal, V.P. Sonam, Seth, N. Kishore, Physica B 365 (2005) 65.
[25] W.A. Pisarski, G. Dominiak-Dzik, W. Ryba-Romanowski, J. Pisarska, J. Alloys Compd. 451 (2008) 220.
[26] W.A. Pisarski, T. Goryuka, B. Wodecka-Dus, B. Plonska, J. Pisarska, Mater. Sci. Eng. B—Solid State Mater. Adv. Technol. 122 (2005) 94.
[27] Y.B. Saddeek, J. Alloys Compd. 467 (2009) 14.
[28] M.A.K. El-Fayoumi, M. Farouk, J. Alloys Compd. 482 (2009) 356.
[29] M. Bengisu, R.K. Brow, E. Yimaz, A. Mogus-Milankovic, S.T. Reis, J. Non-Cryst. Solids 352 (2006) 3668.